Extreme set-up and run-up on steep cliffs (Banneg Island, France)

Fabrice Ardhuin, Lucia Pineau-Guillou, Bernard Fichaut, Serge Suanez, David Corman, Jean-François Filipot

HAL Id: hal-00665924
https://hal.archives-ouvertes.fr/hal-00665924

Submitted on 10 Aug 2014

EXTREME SET-UP AND RUN-UP ON STEEP CLIFFS
(BANNEG ISLAND, FRANCE)

Fabrice Ardhuin[1], IFREMER, Laboratoire d'Oceanographie Spatiale, Plouzané, FRANCE
Lucia Pineau-Guillou, IFREMER, DYNECO/PHYSED, Plouzané, FRANCE

Bernard Fichaut and Serge Suanez, LETG-Géomer-Brest, IUEM, Plouzané, France

David Corman and Jean-François Filipot
Service Hydrographique et Océanographique de la Marine, Brest, France

1 Introduction

Waves and water levels are the dominant factors shaping coastal morphology, be it at river mouths [e.g. Friedrichs and Wright, 2004], or over steep rocky shorelines [e.g. Hansom and Hall, 2009]. instantaneous (run-up) are also highly important for human activities. The infrequent high water levels, associated with strong storms and spring tides, are equally important for the coastal geomorphological evolution and the general safety of coastal activities. Many studies on gently sloping beaches have shown that empirical predictors of set-up and run-up level [e.g. Stockdon et al., 2006], can actually be more accurate than deterministic models based on hydrodynamic models using radiation stresses [Apotsos et al., 2007]. Here we focus on natural steep cliffs, for which few observations have been published. This study was performed because we wanted to understand the overwash and amazing cliff-top deposits of Banneg island reported by Fichaut and Suanez [2011], and illustrated on figure 1.

We found it very difficult to apply empirical formulas for set-up and run-up mostly calibrated for smaller sloping shore-faces, with different topographies. A dedicated field measurement campaign povided measurements that we used to establish a very accurate proxy for the water level in terms of wave parameters (correlation r 0.94). This local empirical parameterization of the water levels is then used to interpret the morphological changes during the March 10, 2008 storm.
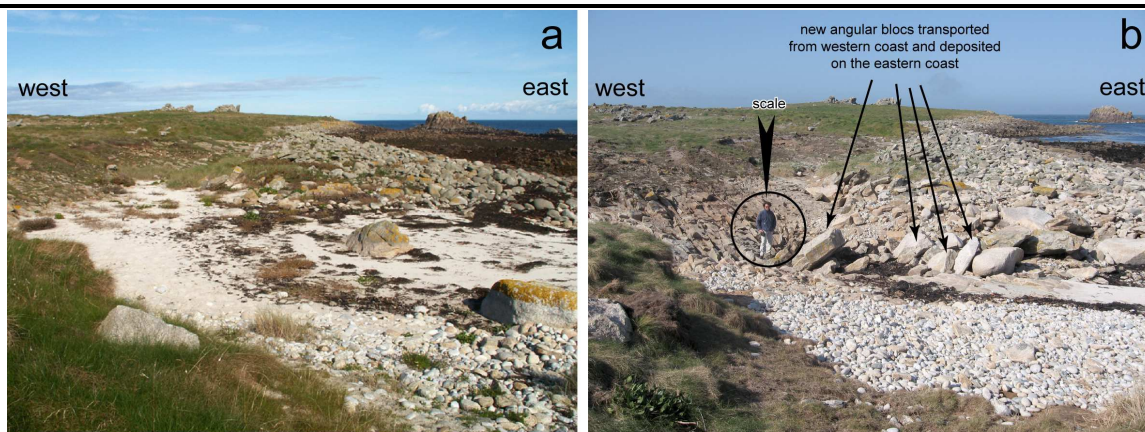

Fig. 1 : Morphological changes in the central part of Banneg Island. Comparison between (d) June 2005 and (e) April 2008 of the area located at the mouth of the gully on the eastern coast of Banneg Island. Note the 1.6 m deep pit dug in the upper sandy beach and deposition of blocks during the storm.

---

[1] E-mail:ardhuin-at-ifremer.fr

2   measurements in Banneg
winter 2008–2009

2.a Island morphology and instrument set-up

Banneg is a small island off the Western French coast, 1 km long and 200 m across, located in the Molène Archipelago, off the western tip of mainland France (figure 2). Although the Island of Ouessant is fully exposed to North Atlantic waves, with maximum significant wave heights (H_s) of the order of 12 m, Banneg is partially sheltered by its bigger neighbor Ouessant.
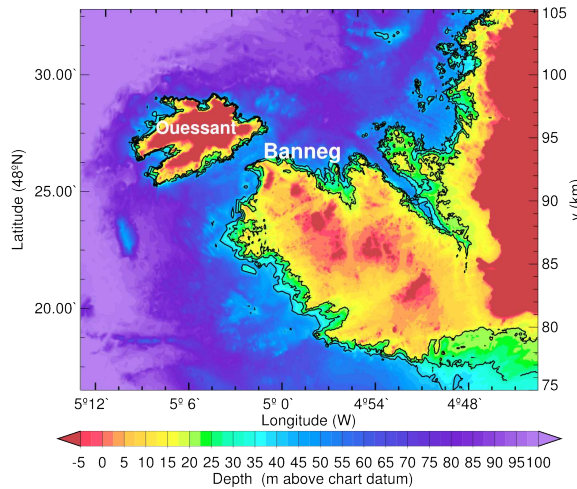

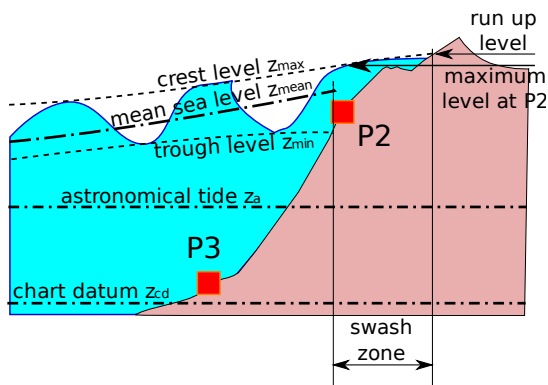Fig. 2 : Bathymetry surrounding the Molne Archipelago (source SHOM, vertical reference is chart datum).

Fig. 3 : Definition of water levels. In this schematic the squares P3 and P2 represent pressure recorders that are used to estimate the mean and instantaneous water levels above them.
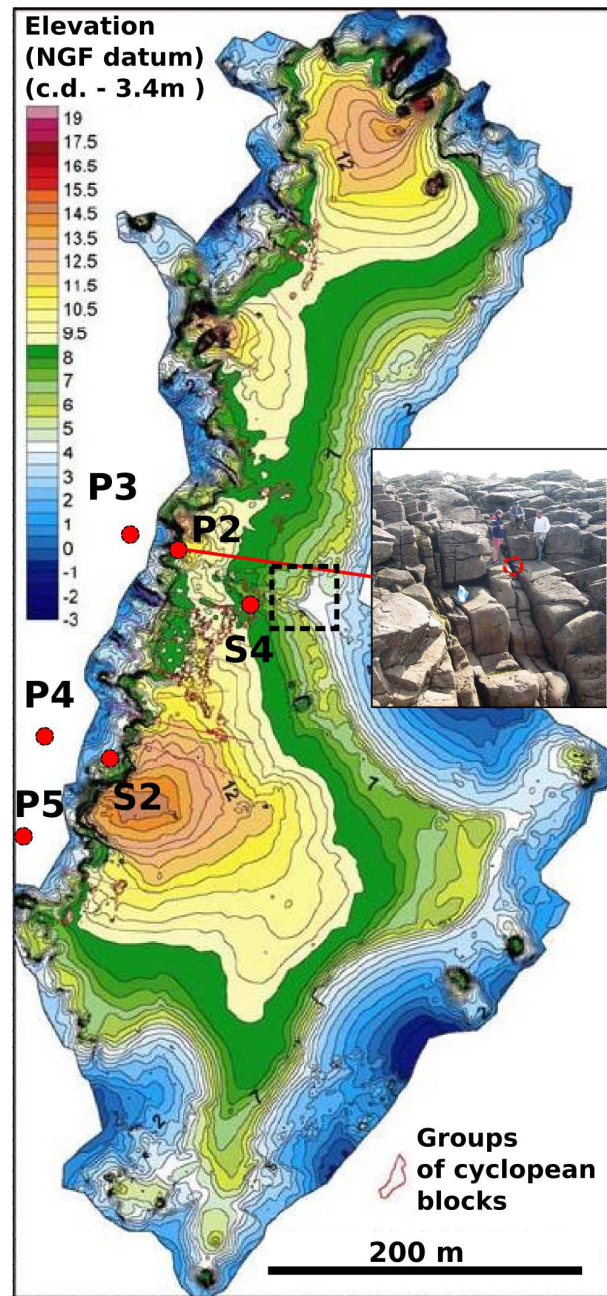
Fig. 4 : Topography of the island of Banneg. The red dots indicate the locations of the pressure sensors deployed in September 2008. The inset picture shows the actual cliff and detailed location of pressure gauge P2 [adapted from Fichaut and Suanez, 2006]. The dashed box is centered on the area pictured in figure 1

Based on numerical wave model results, the west coast of Banneg is exposed to waves that are typically 40% smaller than those found offshore. Cliff on its western shore have slopes between 0.3 and 3,

and the lowest points along the cliff crest are 5 meters above the highest predicted tide, which is 10 m above mean sea level. At the top of these slopes, the rock is fractured (see inset picture on figure 4) and cyclopean blocks are quarried during severe storms, and transported all the way across the island, which can be 200 m.

Several pressure gauges (P2 to P5: Ocean Sensor System model OSSI-010-003C; S2 and S4: HOBO water level gauge) were mounted on stainless steel plates bolted into the rock using chemical fixings, with the exception of S4 which was located in a small house and used to record atmospheric pressure. Here we will use results from two sensors P3 and P2 which are installed along a cross-shore transect, at elevations 1.30 and 7.52 m above chart datum. The recorded pressure was converted to water elevation by subtracting the atmospheric pressure measured by sensor S4, and assuming hydrostatic equilibrium with a water and air densities estimated from the recorded temperature.

Other sensors were installed in the southern part of the island, providing five time series of water elevation above each. All the data from P2, P3, P4 and P5 were sampled at 5 Hz, data from S2 was sampled at 2 minute intervals. Here we will focus on data from P3 and P2.

2.b Mean water levels

Time series of 1-minute maxima are shown in figure 5, showing the well known local tide properties with dominant M_2 and S_2 constituents, giving a neap/spring tidal cycle of 14 days with amplitudes ranging from 2 to 7 m. The very good overlap of all sensors shows the good quality of the data without any significant drift over the measurement period.
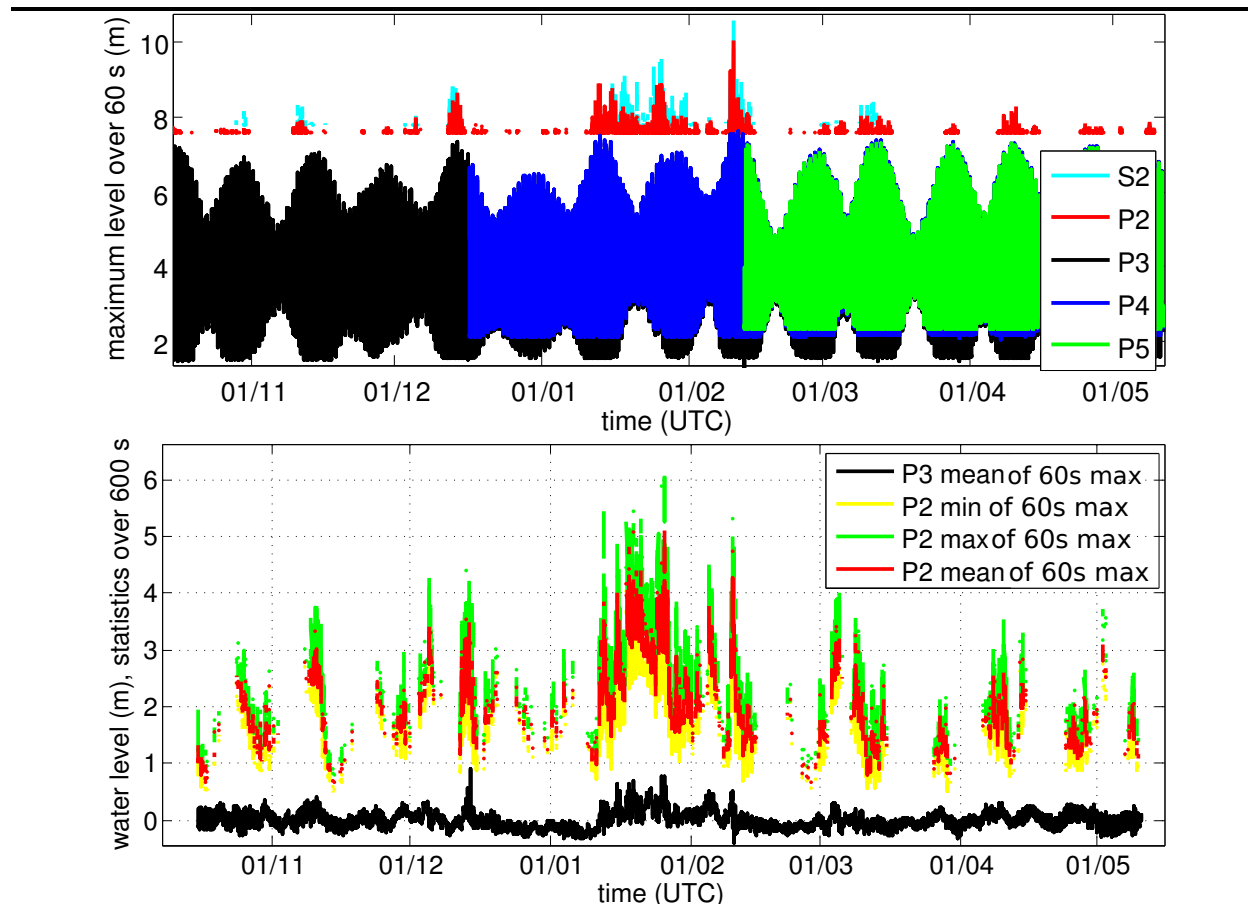

Fig. 5 : Top panel: 1-minute averages for the five water level times series from October 2008 to May 2009, relative to chart datum. Bottom panel, 10-minute minima and maxima at P3 and P2 from the 1-minute maxima. The predicted tide has been removed.
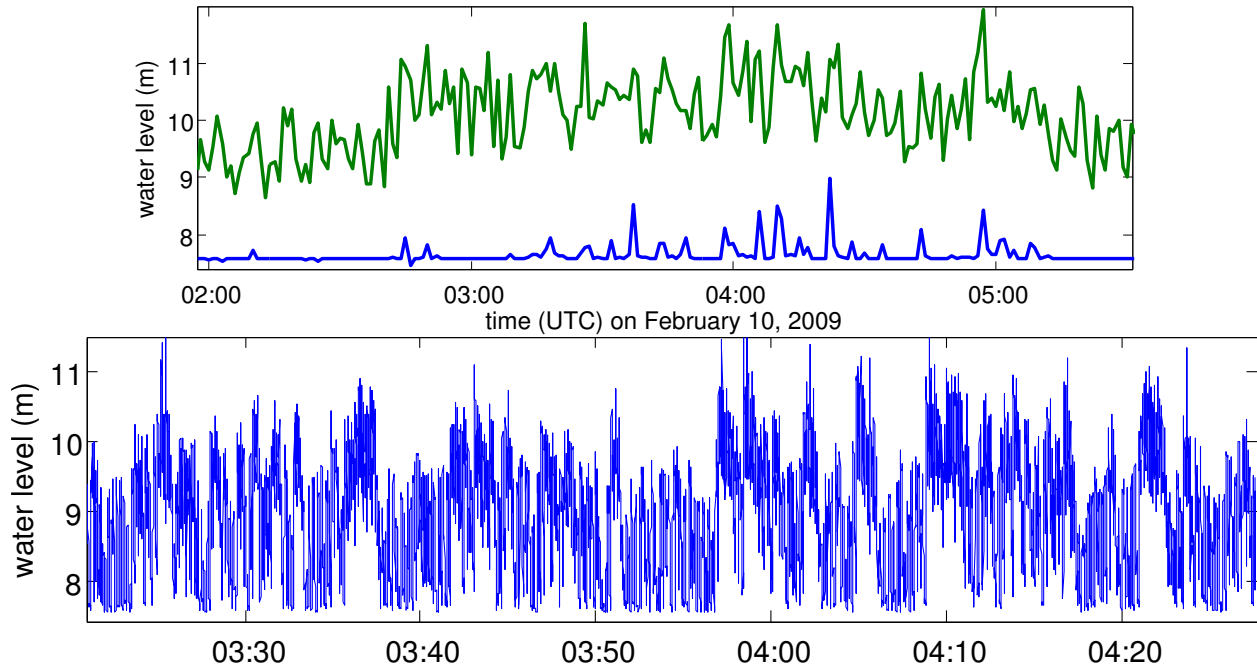
3

Fig. 6 : Top panel: 1-minute minimum and maximum water levels recorded at P2 around the time of the highest water level. Bottom panel, full water level series for one hour.

This time series also shows that P_2 lies above the maximum predicted tide, but it gets wet fairly often during winter at high tide, in particular in January and February, and occasionally also in October and May.

The predicted tide was estimated with two methods, the T-tide package Pawlowicz et al. [2002] and the species concordance method of Simon [2007]. For our 6-month long record the difference between the two methods is small, but the lowest residual was obtained with latter method which was thus chosen. The residuals for gauges P3 and P2 are shown in figure 5.

We particularly focus on the highest sensor P_2. Because this is dry most of the time, it is difficult to define a mean water level at P_2, in fact, there are very few occasions when both the 1-minute minima and maxima show that the sensor has been continuously under water for at least one minute. The only time when this happened was on the morning high tide of February 10, 2009. Figure 6 shows the 1-minute minimum and maximum levels at P2 as well as the full time series at P2 between 3:25 and 4:25 UTC. A close examination of that time series shows that there are a few events, lasting for 1 to 3 minutes during which the water level stays very high, for ex-

ample around 4:10 UTC.

Because the instrument was positioned to minimize the direct impact of water on the sensor, there is no reason to believe that there are particular biases in the record. In fact, the joint examination of P3 and P2, in figure 7, reveals several interesting features. First of all, there is no obvious correlation between the water levels recorded by the two instruments, which is rather surprising given the short distance between them (about 30 meters). On a closer inspection there is a systematic drop in water level at P3 at the end of each high water event at P2, for example at 4:11:15. Also, the high water events at P2 appear to be rather associated with smaller wave heights at P3, suggesting that these motions are associated with bound long waves [Munk, 1949]. Yet, the very abrupt rise in water level at the beginning of each event, sometimes more than 2 m in less than 1 s, is very unusual, and will require further measurements with more instruments to understand how the water is climbing up the cliff.

From 4:09 to 4:11 the mean water level difference between P3 and P2 is 2.46 m, and the water level at P3 is 0.5 m above the predicted tide. As a result the mean water level at P2 is 3.0 m above the predicted tide, possibly the highest level recorded
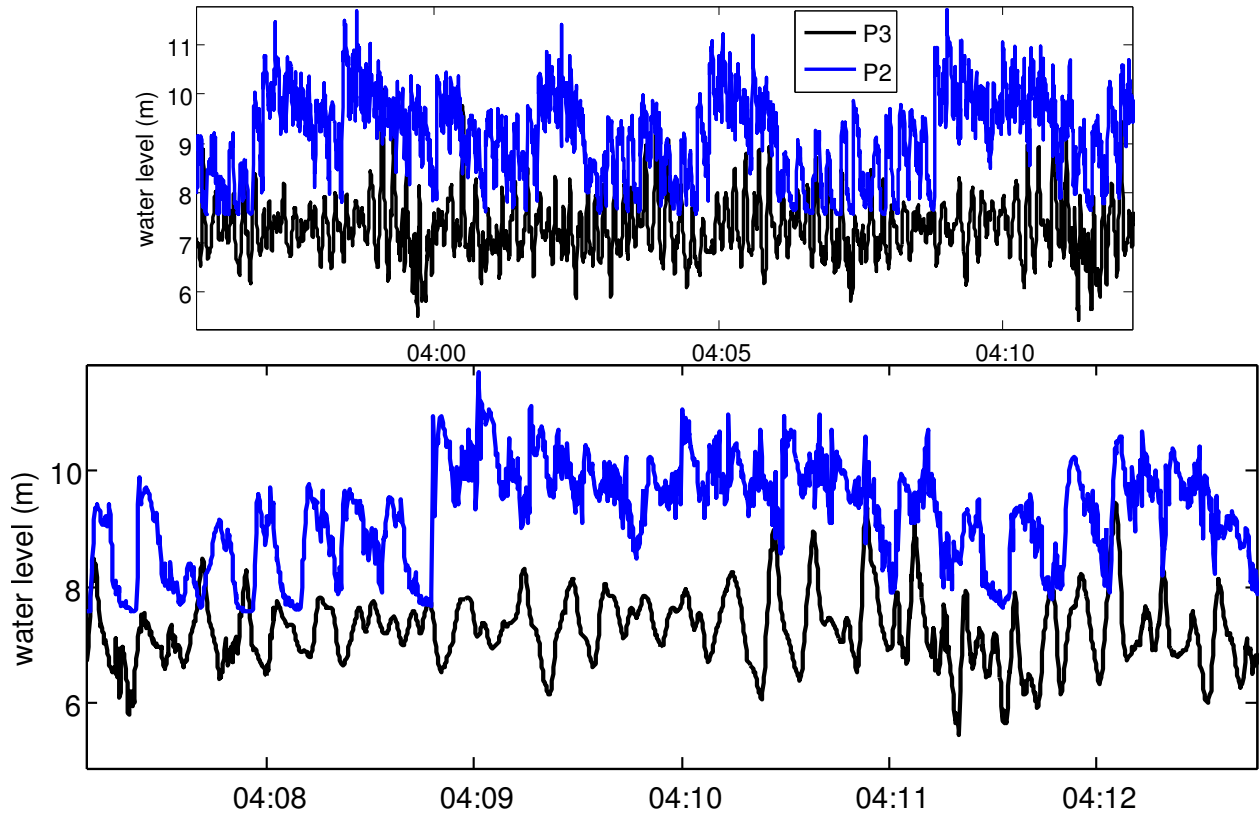
Fig. 7 : Full time series of water levels at P2 and P3, relative to chart datum. This is an elarged view of part of the time series shown in 6.

on the coasts of France. At that time the significant wave height offshore of Banneg was estimated to be 4 m, based on a numerical wave model. A very simple one-dimension model for the water level based on radiation stresses [e.g. Raubenheimer et al., 2001], assuming along-shore uniform topography, is useful for putting these values in perspective. Figure 8 shows the results obtained with a much larger offshore wave height.

2.c Offshore waves and maximum water levels
Given the difficulty to define mean water level with instruments that are only part of the time underwater, we will now examine the values of the maximum levels. Contrary to previous studies with video imagery [Stockdon et al., 2006], the use of pressure sensors does not allow a direct measurement of the run-up, defined as the elevation at which the maximum crest level meets the topographic profile. Yet, for surging breakers, it is expected to be above the maximum pressure recorded within one wavelength from the high water line, as represented on figure 3.
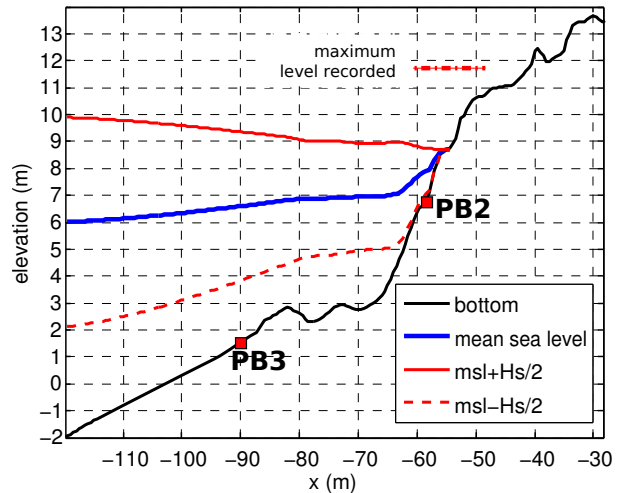

Fig. 8 : Example calculation of significant wave heights and mean water level assuming an along-shore uniform topography.

Calculations were performed with the WAVE-

WATCH III[(R)] modeling framework [Tolman, 2008, 2009], hereinafter WWATCH, including wave generation and dissipation parameterizations by Ardhuin et al. [2010], and the use of advection schemes on unstructured grids [Roland, 2008]. The model calculations are thus identical to the ones performed by Ardhuin et al. [2009], using wind forcing from ECMWF analyses, and now including water levels and currents estimated by one-way nested models using the MARS model developed at Ifremer, with a highest resolution of 300 m and a time resolution that we limit here to 1 hour (15 minutes is available for the finest grid). Water levels at a location 500 m offshore of Bannec was verified to follow our measurements at P3 with a root mean square (rms) error of 20 cm.

Given the location of Banneg, the use of a numerical wave model is needed to, at least, estimate the sheltering effect of the island of Ouessant (figure 10), and the effects of the very strong tidal currents between Ouessant and Banneg.

Although no wave measurements are available at that site, the quality of the model has been verified in several other studies [Ardhuin et al., 2010], and we further verified that the observations at the Pierres Noires buoy (WMO number 62069, see figure 10), are well reproduced by the model. Considering the times between January 25 and March 31, 2008, Pearson's correlation coefficient between hourly model output and hourly buoy data is $r = 0.980$ for H_s, with a normalized rms error (NRMSE) of 10.8% only. These numbers improve to $r = 0.984$ and NRMSE=9.9% when the buoy data is averaged over 3 hours Again for data averaged over 3 hours, the model agrees very well with measured mean periods $T_{m0,2}$ ($r = 0.92$ and NRMSE=11.4%) and $T_{m0,-1}$ ($r = 0.91$ and NRMSE=7.9%). This excellent level of agreement, is typical of open ocean conditions [Rascle et al., 2008]). Compared to previous simulations without current by Ardhuin et al. [2009], the model is much more accurate, and reproduces the observed tidal modulation of wave parameters, although with a reduced amplitude. This suggests that the model can be used a a good source of wave parameters just offshore of Banneg, even though the stronger current there may introduce slightly larger errors.

Indeed, we find a very good correlation between a model-derived Hunt parameter $H_H = T_{m0,-1}\sqrt{gH_s}$ [Hunt, 1959], estimated at a location 500 m to the west of Banneg, and the recorded water levels (figure 9). Taking all the data with a time resolution

of 10 minutes, Pearson's correlation coefficient is $r = 0.90$). As expected, the water levels are also a function of the predicted tidal level, since the bottom slope felt by the wave will vary with the water elevation. Here the water elevation above P2 generally increases for decreasing levels of the predicted tide.

This empirical fit is similar to the expression given by Stockdon et al. [2006] for reflective beaches, in their eq. (20), which can be re-written as

$$z_{2\%} = 0.91\beta_f T_{m0,-1}\sqrt{gH_s} \qquad (1)$$

where β_f is the foreshore slope. Their expression coincides with ours if we take $\beta_f = 0.081$, which would have been rather difficult to guess from the cliff profile, and appears rather low compared to the actual slopes which are rather of 0.4 on average. This suggests that such empirical formulas may not be applicable to the steep slopes encountered here.

3 Expected water levels on March 10, 2008
This present study was largely motivated by the extreme morphogenic event associated with the March 10, 2008 storm. This event was most severe in recent years in terms of wave heights and coincided with a high spring tide, causing widespread damage along the Western French coasts [Cariolet et al., 2010] and and important impacts on Banneg. The motion of large blocks across the island is well documented by Fichaut and Suanez [2011].
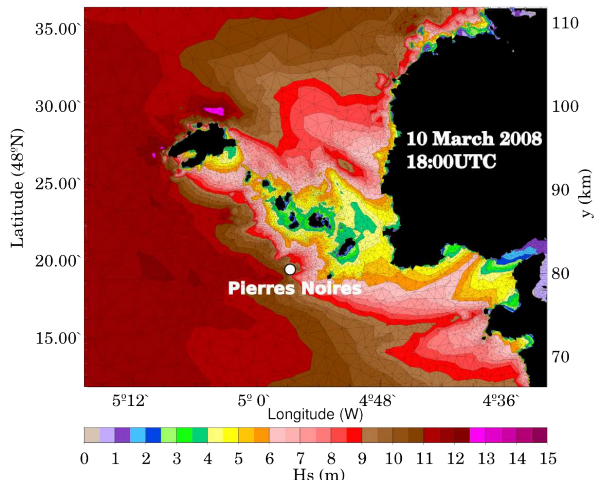

Fig. 10 : Map of wave heights predicted for March 10, 2008, 18:00 UTC. For this North-Westerly storm, the wave heights just in front of Banneg are reduced by about a factor 2 compared to wave heights offshore of Ouessant.
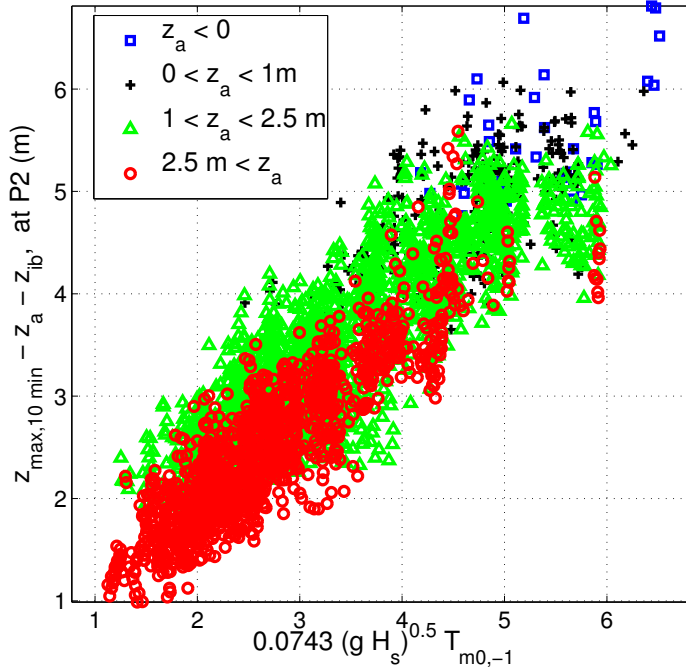
6

Fig. 9 : Maximum water level minus predicted tide z_a and inverse barometer z_{ib} at P2 as a function of the modeled Hunt parameter offshore of Banneg island.

We will base our estimation of the maximum water levels at the location of the P2 wave gauge on the empirical relationship fitted on the winter 2008-2009 data, namely

$$z_{\max} = z_a + z_{\text{ib}} + 0.0743 T_{m0,-1}\sqrt{gH_s}. \quad (2)$$

With a much larger wave height, $H_s = 6.76$ m in front of Banneg instead of 4.53 m on February 10, 2009, and a much larger mean wave period, $T_{m0,-1} = 13.2$ s instead of 9.0 s, the March 10, 2008 storm is expected to have produced a maximum water level 3.6 m higher than the maximum value that we have recorded, easily going over the top of the cliff (see figure 8).

There is a fair amount on uncertainty in this estimate as we have seen than the empirical coefficient 0.0743 in eq. (2) is probably a function of the water level, but it gives an indication of the much larger expected water level.

4   Conclusions

Measurements of water levels on the exposed cliff of Banneg island (archipel de Molène, France) were performed in the winter 2008–2009 to investigate the relation between storms and extreme water levels that lead to the quarrying of blocks from the top of

the cliff and their deposition across the island, with the most extreme event recorded in March 2008.

The recorded water levels clearly show that mean water levels are highly variable during storms, with a complex pattern across the cliff profile that suggests a three-dimensional flow. Averaged over 2 minutes, the highest water level was recorded 3.0 m above the predicted tide on February 10, 2009. This event was associated with a rather moderate storm. Our six months of recording reveal that the maximum water levels on the cliff are tightly related to a Hunt parameter $H_H = T_{m0,-1}\sqrt{gH_s}$ [Hunt, 1959], with a correlation $r = 0.94$ once the variability of water levels is corrected for. Our records include a maximum water level of 6.6 m relative to the tide.

Extrapolating these values to the March 10 2008 storm, we find a maximum water level 8.0 m above the predicted tide. Combined to the spring tide of that day, with the same value as on February 10, 2009, the expected maximum water level was probably 1.5 m above the top of the cliff, explaining the torrential flows that are evidenced by the removal of the thick grass layer in the central part of the island, and the complete erosion of the sand beach on the sheltered side of the island where a large mound of

1–2 m diameter blocks have been assembled (figure 1).

The steep slope of the cliff and the relatively deep water offshore are responsible for particularly high water levels. It appears that empirical formulas fitted on beaches do not predict well the observed water levels. The island probably owes its survival to the partial shelter offered by the bigger island of Ouessant.

References

A. Apotsos, B. Raubenheimer, S. Elgar, R. T. Guza, and J. A. Smith. Effects of wave rollers and bottom stress on wave setup. *J. Geophys. Res.*, 112:C02003, 2007. doi: 10.1029/2006JC003549.

F. Ardhuin, L. Marié, N. Rascle, P. Forget, and A. Roland. Observation and estimation of Lagrangian, Stokes and Eulerian currents induced by wind and waves at the sea surface. *J. Phys. Oceanogr.*, 39(11): 2820–2838, 2009. URL http://journals.ametsoc.org/doi/pdf/10.1175/2009JPO4169.1.

F. Ardhuin, E. Rogers, A. Babanin, J.-F. Filipot, R. Magne, A. Roland, A. van der Westhuysen, P. Queffeulou, J.-M. Lefevre, L. Aouf, and F. Collard. Semi-empirical dissipation source functions for wind-wave models: part I, definition, calibration and validation. *J. Phys. Oceanogr.*, 40(9):1917–1941, 2010.

J.-M. Cariolet, S. Costa, R. Caspar, F. Ardhuin, R. Magne, and G. Goasguen. Atmospheric and marine aspects of the 10th of march 2008 storm in atlantic and in the Channel. *Norois*, 215, 2010. In French.

B. Fichaut and S. Suanez. Amas de blocs cyclopéens sur l-île de Banneg (Archipel de Molène-Finistère). etude morpho-sédimentaire et dynamique de mise en place. In *Actes des IXèmes journées Génie côtier-Génie civil, Landeda*. Centre Français du Littoral, 2006.

B. Fichaut and S. Suanez. Quarrying, transport and deposition of cliff-top storm deposits during extreme events: Banneg island. *Marine Geology*, pages 36–55, 2011.

C. T. Friedrichs and L. D. Wright. Gravity-driven sediment transport on the continental shelf: implications for equilibrium profiles near river mouths. *Coastal Eng.*, 51:795–811, 2004.

J. Hansom and A. Hall. Magnitude and frequency of extra-tropical North Atlantic cyclones: a chronology from cliff-top storm deposits. *Quaternary International*, 195:42–52, 2009.

I. A. Hunt. Design of seawalls and breakwaters. *Journal of Waterways and Harbours Division*, 85:123–152, 1959.

W. H. Munk. Surf beat. *Eos Trans. AGU*, 30:849–854, 1949.

R. Pawlowicz, B. Beardsley, and S. Lentz. Classical tidal harmonic analysis including error estimates in MATLAB using T_TIDE. *Computers and Geosciences*, 28:929–937, 2002.

N. Rascle, F. Ardhuin, P. Queffeulou, and D. Croizé-Fillon. A global wave parameter database for geophysical applications. part 1: wave-current-turbulence interaction parameters for the open ocean based on traditional parameterizations. *Ocean Modelling*, 25:154–171, 2008. URL http://hal.archives-ouvertes.fr/hal-00201380/. doi:10.1016/j.ocemod.2008.07.006.

B. Raubenheimer, R. T. Guza, and S. Elgar. Field observations of wave-driven setdown and setup. *J. Geophys. Res.*, 106(C3):4629–4638, 2001.

A. Roland. *Development of WWM II: Spectral wave modelling on unstructured meshes.* PhD thesis, Technische Universität Darmstadt, Institute of Hydraulic and Water Resources Engineering, 2008.

B. Simon. *La marée océanique côtière.* Institut Océanographique, 2007.

H. F. Stockdon, R. A. Holman, P. A. Howd, and A. H. Sallenger, Jr. Empirical parameterization of setup, swash, and runup. *Coastal Eng.*, 53:573–588, 2006.

H. L. Tolman. A mosaic approach to wind wave modeling. *Ocean Modelling*, 25:35–47, 2008. doi: 10.1016/j.ocemod.2008.06.005.

H. L. Tolman. User manual and system documentation of WAVEWATCH-III^{TM} version 3.14. Technical Report 276, NOAA/NWS/NCEP/MMAB, 2009. URL http://polar.ncep.noaa.gov/mmab/papers/tn276/276.xml.